J. Biochem. **136**, 693–699 (2004)
DOI: 10.1093/jb/mvh176

Kinetic Analysis of Precursor M1 RNA Molecules for Exploring Substrate Specificity of the N-Terminal Catalytic Half of RNase E

Kwang-sun Kim[1], Soyeong Sim[1,*], Jae-hyeong Ko[1], Bongrae Cho[2] and Younghoon Lee[1,†]

[1]Department of Chemistry and Center for Molecular Design and Synthesis, Korea Advanced Institute of Science and Technology, Daejeon 305-701, Korea; and [2]Department of Chemistry, Chongju University, Chongju 360-764, Korea

Received July 30, 2004; accepted September 9, 2004

To gain insight into the mechanism by which the sequence at the *rne*-dependent site of substrate RNA affects the substrate specificity of *Escherichia coli* RNase E, we performed kinetic analysis of the cleavage of precursor M1 RNA molecules containing various sequences at the *rne*-dependent site by the N-terminal catalytic half of RNase E (NTH-RNase E). NTH-RNase E displayed higher K_m and k_{cat} values for more specific substrates. The retention of single strandedness at the *rne*-dependent site was essential for cleavage efficiency. Moreover, the loss of single-strandedness was accompanied by a decrease in both the K_m and k_{cat} values.

Key words: kinetic parameters; M1 RNA, RNase E, *rne*-dependent site, substrate specificity.

Abbreviations: C-terminal half, CTH, N-terminal half, NTH, ribonuclease, RNase.

RNase E, which was initially identified during the processing of 5S rRNA from the 9S rRNA precursor in *Escherichia coli* (*1*), is an essential 118-kDa protein of 1,061 amino acid residues (*2*, *3*). The importance of this enzyme in RNA processing, cell viability, and decay of mRNA is well characterized (*4–8*). Since RNase E is involved in both RNA processing and degradation, substrate discrimination by RNase E is essential for its cellular functions. RNase E can be divided into two functionally distinct regions: an N-terminal half (NTH) containing residues 1–498, and a C-terminal half (CTH) involving residues 499–1061. NTH-RNase E carries the catalytic activity of the enzyme (*9*) and has high sequence similarity to the *E. coli* RNase G protein (*10*). On the other hand, CTH-RNase E contains an arginine-rich RNA binding domain (*9*, *11*) and functions as a platform for the assembly of the *E. coli* degradosome complex (*12–14*).

A consensus sequence of [A/G]AUU[A/U], designated the *rne*-dependent site, is recognized and cleaved by RNase E (*15*). This site has been reported to be located in a single-stranded region rich in U and A nucleotides (*16–18*). However, no simple relationship has been established between the sequence and cleavage efficiency. A number of reports show that the primary sequence at the *rne*-dependent site is insufficient to account for cleavage specificity by RNase E (*19–22*). Other investigators have demonstrated that secondary structures such as stem-loops control susceptibility to RNase E cleavage, possibly by altering the single-strandedness of the binding site or its accessibility to the site (*23–25*).

M1 RNA of 377 nucleotides, the catalytic subunit of RNase P (*26*), is generated by processing precursor M1 RNA (pM1 RNA) of 413 nucleotides and, to a lesser extent, 414 nucleotides (*27–31*). We recently reported that RNase E directly participates in M1 RNA processing, although unidentified cellular factors are required to control complete maturation (*32*). A pentanucleotide, GAUUU, identified as an *rne*-dependent motif, is positioned immediately 3′ to the processing site of pM1 RNA (*30*) and it matches well with the consensus sequence, [A/G]AUU[A/U] (*15*). This sequence functions as a major factor for determining processing efficiency of pM1 RNA *in vivo* and in *in vitro* experiments using cell extracts (*30*, *33*). Although the importance of the *rne*-dependent site for RNase E cleavage has been recognized, little is known about the mechanistic basis for substrate specificity. To gain insight into this mechanism, in the present study, we analyzed cleavage of *rne*-dependent site variants of p23 RNA (*30*), a truncated pM1 RNA, by NTH of RNase E. Our results provide a step towards elucidating the mechanistic basis for target specificity of RNase E, and the role of the *rne*-dependent site in this process, which is a prerequisite for understanding multifunctional roles of RNase E in RNA metabolism within the cells.

MATERIALS AND METHODS

Bacterial Strains and Plasmid—E. coli JM109 (*34*) was used for the construction of plasmids. *E. coli* BL21(DE3) (*35*) was the strain utilized to express recombinant NTH-RNase E. Plasmid pSPd23 contains the SP6 promoter linked to the 5′-end of the internally deleted M1 RNA coding sequence, and a *Dra*I site at position +415 (*30*). Plasmids pSP-RNE(GUUUU) and pSP-RNE(UUUUU) are derivatives of pSPd23 containing the corresponding mutations at the *rne*-dependent site (*32*). The pSP-DN1 plasmid is another derivative of pSPd23 with mutations at the terminator region that disrupt the stem structure

[*]Present address: Department of Cell Biology, Howard Hughes Medical Institute, Yale University School of Medicine, New Haven, Connecticut 06536, USA.
[†]To whom correspondence should be addressed. Tel: +82-42-869-2832, Fax: +82-42-869-2810, E-mail: Younghoon.Lee@kaist.ac.kr

Table 1. **Oligonucleotides used for site-directed mutagenesis.**

Plasmids	Oligonucleotides*
pSP-RNE(UUUUU)-DN1	GGTCAGTTTCACCT**TTTTT**ACGGTTTAACCCGC
	GCGGGTTAAACCGT**AAAAA**AGGTGAAACTGACC
pSP-RNE(UUUUU)-DN3	CTTTTTTACGT**ATATA**CCCGCTTCGGC
	GCCGAAGCGGG**TATAT**ACGTAAAAAAG
pSP-RNE(UUUUU)-DN34	CGCTTCGGCGGG**TATAT**GCTTAAAAGGG
	CCCTTTTAAAGC**ATATA**CCCGCCGAAGCG
pSP-RNE(AAUUU)	GGTCAGTTTCACCT**AA**TTTACGTAAAAAC
	GTTTTTACGTAAA**TT**AGGTGAAACTGACC
pSP-RNE(CAUUU)	GGTCAGTTTCACCT**CA**TTTACGTAAAAAC
	GTTTTTACGTAAA**TG**AGGTGAAACTGACC
pSP-RNE(UAUUU)	GGTCAGTTTCACCT**TA**TTTACGTAAAAAC
	GTTTTTACGTAAA**AT**AGGTGAAACTGACC

*Specific mutagenic primers (listed in the 5′ to 3′ direction) were designed at http://labtools.stratagene.com/QC. Mutations are depicted in bold.

(*30*). pRNEN is an expression plasmid for NTH-RNase E (*32*).

Expression of Recombinant NTH-RNase E—His-tagged NTH-RNase E was expressed using BL21(DE3) cells containing pRNEN, and the resulting recombinant protein was purified, as described previously (*32*).

Site-Directed Mutagenesis—Site-directed mutagenesis at the *rne*-dependent site or/and other sites was performed according to the QuikChange® Site-Directed Mutagenesis kit protocol (Stratagene). The oligonucleotides used for constructing mutant plasmids are summarized in Table 1. Plasmid pSP-RNE(UUUUU)-DN1 was generated using pSP-DN1 as a template. The templates for pSP-RNE(UUUUU)-DN3 and pSP-RNE(UUUUU)-DN34 were pSP-RNE(UUUUU) and pSP-RNE(UUUUU)-DN3, respectively. The pSP-RNE(AAUUU), pSP-RNE(CAUUU), and pSP-RNE(UAUUU) plasmids were generated using pSPd23 as a template.

RNA Substrate Preparation—*Dra*I-linearized plasmids employed in this study were used as templates for *in vitro* synthesis of p23 RNA variants by SP6 RNA polymerase (*33*). For RNase H probing, *in vitro* transcripts were labeled at the 3′-end with [^{32}P]pCp and T4 RNA ligase. In addition, *in vitro* transcripts were internally labeled with [α-^{32}P]CTP for RNase E cleavage assay, as described (*36*).

RNase E Cleavage Assay—The RNA substrate (0.2 pmol) was incubated with purified NTH-RNase E (10 ng) in RNase E buffer (50 mM Tris-HCl, pH 7.5, 20% (v/v) glycerol, 1 mM EDTA, 0.5 M NaCl, 0.5% Triton X-100) in a total volume of 50 μl. The mixture was incubated at 30°C. At the end of reaction, reaction products were extracted with phenol:chloroform:isoamyl alcohol (25:24:1), ethanol-precipitated, and dissolved with 10 μl of sequencing gel loading buffer. Samples were heated at 85°C for 5 min, chilled on ice, and loaded onto 5% polyacrylamide sequencing gels containing 8 M urea. Quantitative analysis was performed using an Image Analyzer BAS1500 (Fuji).

Kinetic Analysis—To determine the steady-state kinetic parameters of RNase E hydrolysis, RNA substrates were incubated with 1 nM NTH-RNase E in RNase E buffer at 30°C for 5 to 20 min. Under these conditions, the initial rate approached its maximum, and less than 30% substrates were converted to processed products. The substrate concentrations varied from 200 nM to 2 μM. Reactions were initiated by the addition of an enzyme diluted in RNase E buffer. Reaction mixtures were incubated in RNase E buffer. The reaction was terminated by adding an equal volume of phenol:chloroform:isoamyl alcohol (25:24:1), and the processed products and remaining substrates were separated on a 5% polyacrylamide/8 M urea sequencing gel. Their amounts were determined by intensity analysis with an image analyzer BAS1500 (Fuji). Kinetic parameters (K_m and k_{cat}) were calculated by non-linear regression fitting of data to hyper 1.1w (a program for the analysis of enzyme kinetic data provided by J.S. Easterby), based on the Michaelis-Menten equation, as shown in Eq. 1.

$$\frac{v}{[E]} = \frac{k_{cat}[S]}{K_m + [S]} \quad (1)$$

Whereby v is the initial rate, [S] is the substrate concentration, and [E] is the total enzyme concentration.

RNase H Probing—For RNase H probing, 0.5 pmol of RNA substrates labeled at the 3′-end with [^{32}P]pCp were preincubated at 37°C for 10 min, then annealed to 10 pmol of oligonucleotides complementary to the region containing the *rne*-dependent site. The oligonucleotides used in the annealing reactions for RNAs were as follows: 5′-GT<u>AAATC</u>AGGT-3′ targeted to GAUUU, 5′-GT<u>AAAAC</u>AGGT-3′ targeted to GUUUU, 5′-GT<u>AAAAA</u>AGGT-3′ targeted to UUUUU, and 5′-GT<u>AGGGC</u>AGGT-3′ targeted to GCCCU. The complementary regions are underlined. When necessary, RNA was heated at 80°C for 10 min and quickly chilled on ice before the annealing reaction to disrupt its secondary structure. Annealing was performed in 20 μl of RNase E buffer at 37°C for 10 min. Hybrids were treated with 0 to 1 unit of RNase H (Promega) for 10 min at 37°C in 50 μl of RNase E buffer. Following phenol:chloroform extraction and ethanol precipitation, RNA was fractionated on a 10% polyacrylamide/8 M urea sequencing gel and visualized by autoradiography.

RESULTS

Kinetic Analysis of Cleavage of Substrates with U-Rich Substitutions at the rne-Dependent Site—We employed p23 RNA, a truncated pM1 RNA, as a model substrate for kinetic analysis of NTH-RNase E (Fig. 1). Based on the

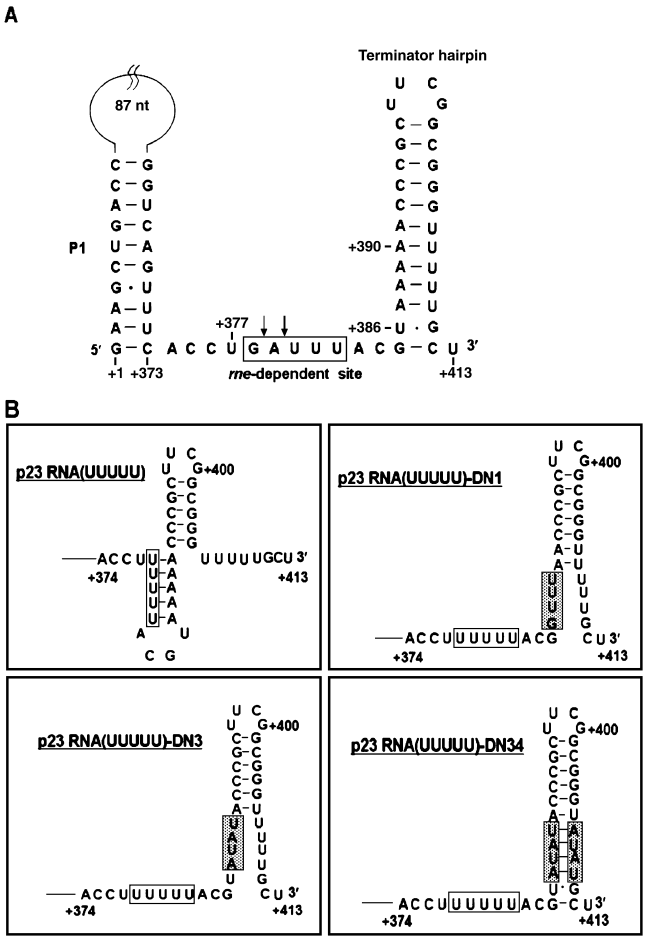

Fig. 1. **p23 RNA variants.** (A) The secondary structure of p23 RNA surrounding the *rne*-dependent site. The arrows signify the minor and major cleavage sites at positions +378 and +379, respectively, by NTH-RNase E (*28*). (B) Possible secondary structures of p23 RNA(UUUUU) variants surrounding the *rne*-dependent site arising from sequence change. The *rne*-dependent site is boxed. Sequence alterations in the terminator stem are also boxed with shaded residues.

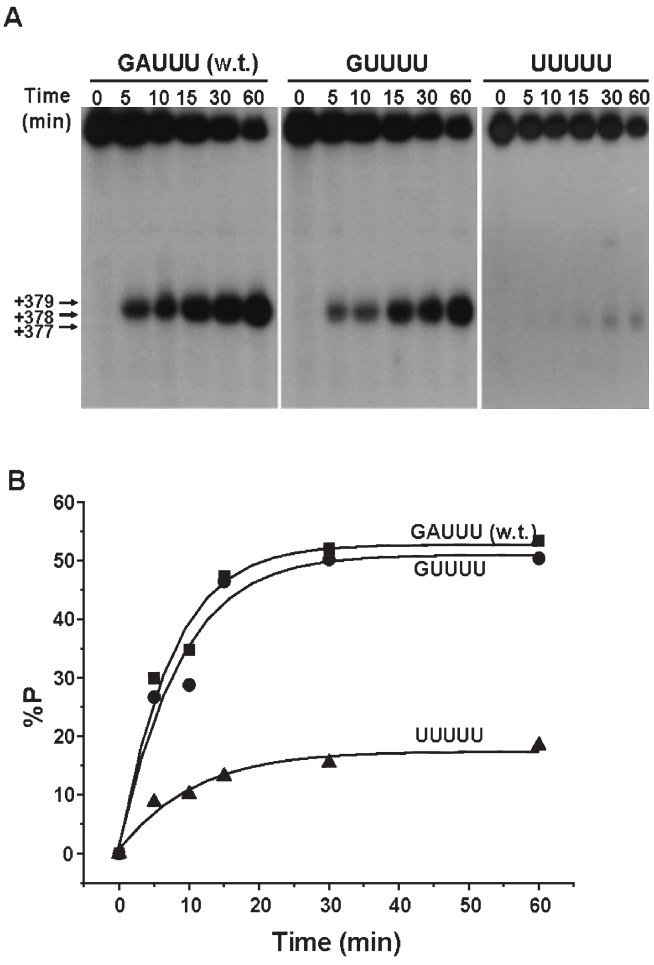

Fig. 2. **Cleavage reaction of p23 RNA variants by NTH-RNase E.** p23 RNA variants at the *rne*-dependent site were internally labeled with [α-^{32}P]CTP. (A) Labeled RNA substrates were incubated at 30°C with purified NTH-RNase E (10 ng). The reaction products were withdrawn at the indicated time-periods and separated on a 5% polyacrylamide sequencing gel. (B) Product conversion percentages (*%P*) were calculated from the ratio of processed RNA to that of total input by quantifying gels with an Image Analyzer.

finding that the sequence of the *rne*-dependent site is recognized by RNase E (*15*), we used variants of p23 RNA mutated at the *rne*-dependent site for determining substrate specificity. In this regard, p23 RNA is an ideal substrate, since a single-stranded region of 11 nucleotides (including the *rne*-dependent site) is flanked by two stable stem structures, specifically, the upstream P1 stem and the downstream terminator stem (Fig. 1; Ref. *30*). Therefore, variations at the *rne*-dependent site are expected to have minimal effects on the maintenance of its single-stranded nature. We previously showed that the *rne*-dependent site of p23 RNA is the major factor determining the efficiency of processing to mature RNA, either in the cell or in *in vitro* experiments using a 40% ammonium sulfate precipitate of the S30 fraction (ASP-40) (*33*). Two U-rich substrates containing the sequences "GUUUU" and "UUUUU" were selected in this study, since their *in vivo* processing efficiencies are similar to that of the wild-type GAUUU sequence (*33*). Initially, the time-course of cleavage by NTH-RNase E was examined (Fig. 2). NTH-RNase E displayed the highest activity for wild-type GAUUU. NTH-RNase E activity on the GUUUU variant was comparable to that for the wild-type. However, the activity of NTH-RNase E on the UUUUU variant was significantly lower. This lower activity is inconsistent with the wild-type level of processing efficiency of the UUUUU derivative *in vivo* (*33*).

We compared the kinetic parameters of the cleavage of the wild-type substrate, GUUUU, and UUUUU derivative (Table 2). As expected, the highest k_{cat}/K_m value was obtained with the wild-type substrate, and the lowest with the UUUUU derivative. Interestingly, both K_m and k_{cat} values were high for the substrate cleaved with higher efficiency.

The possible loss of single-strandedness at the *rne*-dependent site of the GUUUU and UUUUU variants might have influenced cleavage efficiencies by NTH-

Table 2. **Kinetic parameters of cleavage of p23 RNA variants containing mutations at the *rne*-dependent site.**

Substrate*	K_m (μM)†	k_{cat} (s^{-1})†	k_{cat}/K_m ($s^{-1}\cdot M^{-1}$)†
GAUUU (wt)	1.235 (±0.112)	0.765 (±0.066)	6.203 (±0.040) × 10^5
GUUUU	0.366 (±0.029)	0.121 (±0.012)	3.264 (±0.013) × 10^5
CAUUU	0.464 (±0.031)	0.150 (±0.007)	3.243 (±0.007) × 10^5
AAUUU	0.725 (±0.020)	0.192 (±0.002)	2.648 (±0.004) × 10^5
UAUUU	0.809 (±0.013)	0.209 (±0.005)	2.580 (±0.009) × 10^5
UUUUU-DN34	0.324 (±0.032)	0.023 (±0.001)	0.726 (±0.005) × 10^5
UUUUU	0.278 (±0.042)	0.015 (±0.001)	0.540 (±0.011) × 10^5

*Substrates are listed with sequences of the *rne*-dependent site by decreasing k_{cat}/K_m values. †All values are averages, based on data from independent assays performed in triplicate.

RNase E, since U-rich sequences can base-pair with the A-rich sequences present in the terminator stem. Thus, we assessed single-strandedness at the *rne*-dependent site in these variants by hybridization with complementary oligonucleotides followed by RNase H treatment, which led to cleavage of single-stranded RNA regions hybridized to the oligonucleotides (Fig. 3). Both the GUUUU variant and wild-type substrate were cleaved at the *rne*-dependent site by RNase H, suggesting that the *rne*-dependent sites maintain single-strandedness. However, the UUUUU variant was not cleaved by RNase H. When the UUUUU variant was heated at 80°C to disrupt its secondary structure, RNase H digested this variant. These findings suggest that single-strandedness of the *rne*-dependent site in the UUUUU variant was lost. It is expected that the UUUUU sequence base-pairs with AAAAA at positions 387 to 391 in the lower part of the terminator stem (Fig. 1B). Accordingly, we introduced the UUUUU sequence at the *rne*-dependent site of p23 RNA-DN1, where the terminator stem has already been mutated to disrupt the structure of this region (Fig. 1B). The resulting variant, p23 RNA(UUUUU)-DN1 (Fig. 1B), was additionally cleaved by NTH-RNase E at a site near position +386 (Fig. 4). This is because the GUUUA sequence introduced by the DN1 mutation functions as a new *rne*-dependent site. The GUUUA sequence was mutated to UAUAU to generate p23 RNA(UUUUU)-DN3 (Fig. 1B). This variant was also cleaved near position +386, but with lower efficiency because of the sequence change at the new *rne*-dependent site (Fig. 4). We introduced another compensatory substitution in the terminator stem that restored base-pairing in the terminator stem of p23 RNA(UUUUU)-DN3. The resulting variant, p23 RNA(UUUUU)-DN34, was exclusively cleaved at the original *rne*-dependent site (Figs. 1 and 4). This finding suggests that loss of single-strandedness at the new *rne*-dependent site made it a poor target. Single-strandedness at the original *rne*-dependent site in p23

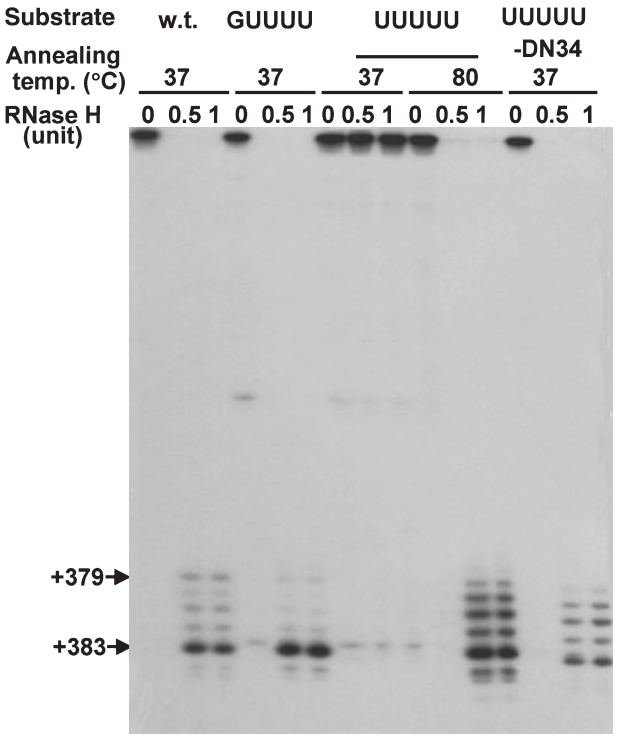

Fig. 3. **RNase H probing of the *rne*-dependent site.** p23 RNA variants labeled with [^{32}P]pCp at the 3′-end were annealed to cognate antisense oligonucleotides, and the resulting hybrids digested with 0 to 1 unit of RNase H. Cleavage products were fractionated on a 10% polyacrylamide sequencing gel. Arrows indicate the positions of cleavage products in RNA substrates.

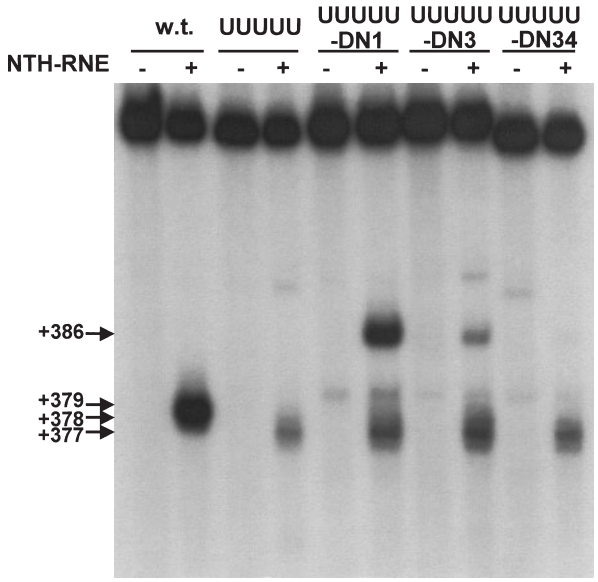

Fig. 4. **Cleavage reaction of p23 RNA-RNE(UUUUU) by NTH-RNase E.** RNA substrates labeled internally with [α-^{32}P]CTP were incubated at 30°C with NTH-RNase E (10 ng) for 30 min. Reaction products were electrophoresed on a 5% polyacrylamide sequencing gel. The positions of the cleavage sites are indicated by arrows.

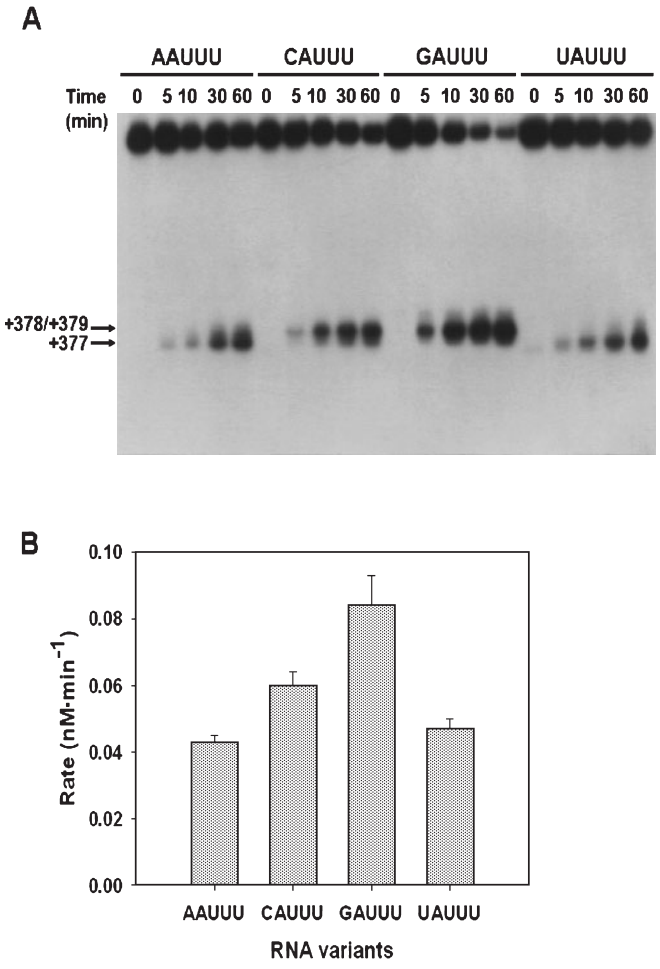

Fig. 5. **Cleavage reaction of G378 variants of p23 RNA by NTH-RNase E.** (A) RNA substrates labeled internally with [α-^{32}P]CTP were incubated at 30°C with NTH-RNase E (10 ng) for 30 min, and products were analyzed on a 5% polyacrylamide sequencing gel. (B) Quantitative analysis of the gel using an Image Analyzer, as described in Fig. 2B. The rate was calculated by dividing the concentration of the processed RNA by the reaction time. All values are averages, based on data from independent assays performed in triplicate.

RNA(UUUUU)-DN34 was confirmed by an RNase H digestion experiment (Fig. 3). p23 RNA(UUUUU)-DN34 was cleaved more efficiently than p23 RNA(UUUUU), indicating that the loss of single-strandedness at the original *rne*-dependent site in p23 RNA(UUUUU) also led to the decrease of cleavage efficiency. Accordingly, all the data suggest that the retention of single-strandedness at the *rne*-dependent site is required for efficient cleavage.

We compared the apparent kinetic parameters of cleavage of p23 RNA(UUUUU) and p23 RNA(UUUUU)-DN34 (Table 2). Higher K_m and k_{cat} values were obtained for p23 RNA(UUUUU)-DN34 that was cleaved with higher efficiency. However, the cleavage of p23 RNA(UUUUU)-DN34 was less efficient than that of the wild-type GAUUU and the GUUUU variant (Table 2). This means that the low cleavage efficiency of the UUUUU variant results from the sequence itself at the *rne*-dependent site. Therefore, we conclude that the UUUUU sequence at the *rne*-dependent site is a poor target for NTH-RNase E.

Effect of G378 Substitution on the Cleavage Rate and Site Selection—The oligonucleotide-based assay revealed that a G nucleotide positioned in close proximity to the scissile bond in the *rne*-dependent site facilitates efficient cleavage by RNase E (*37*, *38*). Although the oligonucleotide-based assay is valuable for probing G-specificity, it is unknown whether this specificity is applicable to naturally occurring RNA substrates. To answer this, we employed p23 RNA as a model RNA substrate. The first G nucleotide of the *rne*-dependent site was replaced with either A, C or U. Time-course experiments were performed with the four substrates (Fig. 5). The G substrate (wild-type) was cleaved most efficiently. The A and U substrates were cleaved least efficiently. On the other hand, the C substrate was cleaved with moderate efficiency. We conclude that G or C is preferable to A or U as the first nucleotide of the *rne*-dependent site. The alteration of the first G nucleotide modified the cleavage site in some cases. The C substrate generated the major processed product with the 3′ end at +379, similar to the wild-type G substrate, while the A and U substrates generated a product with the 3′ end at +377. This result is consistent with *in vitro* data on ASP-40 showing that variants with A/U at the first nucleotide at the *rne*-dependent site generate +377/+378 products, while the wild-type substrate produces +378/+379 products (*33*). We additionally compared the apparent kinetic parameters of these first nucleotide variants (Table 2). The order of k_{cat}/K_m and for the four substrates is GAUUU>CAUUU>AAUUU ≅UAUUU, as expected. Again, the substrates with higher k_{cat} consistently displayed higher K_m values.

DISCUSSION

Precursor M1 RNA has an rne-dependent site downstream of the processing site. Sequence variation at this site affects substrate specificity within the cell or under *in vitro* conditions (*30*, *33*). We previously showed that RNase E is directly involved in this processing (*32*). Therefore, RNase E is responsible for determining substrate specificity, according to the sequences at the *rne*-dependent site. In this study, as an initial step in understanding the mechanism by which substrate specificity of RNase E is determined, we performed kinetic analysis of the cleavage of rne-dependent site variants of p23 RNA, as a natural substrate, by NTH of RNase E. The wild-type GAUUU sequence was cleaved efficiently among the variants tested, with the highest K_m and k_{cat} values. Substrates with higher K_m values had higher k_{cat} values. Studies using partially purified RNase E activities for T4 gene *32* and *rpsT* mRNA substrates have suggested that single-strandedness at the *rne*-dependent site is important for efficient cleavage (*15*, *20*, *21*). Here we confirmed the importance of single-strandedness at the *rne*-dependent site using the purified NTH-RNase E. The loss of single-strandedness at the *rne*-dependent site led to decreased cleavage efficiency with decreased K_m and k_{cat} values. Therefore, the rule that substrates with higher K_m have higher k_{cat} is also applicable to those with different structures at the same *rne*-dependent site.

The UUUUU derivative is a poor substrate for NTH-RNase E. However, this derivative is processed with the same efficiency as the wild-type *in vivo*. The reason for this discrepancy between *in vitro* and *in vivo* cleavage efficiency remains to be clarified. It is known that cellular factors are required for modifying the cleavage site specificity of NTH-RNase E (*32*). Similarly, other unidentified factors may be involved in the processing of this U-rich substrate. However, RNase G, a homolog of NTH-RNase E, does not seem to be involved in processing the UUUUU substrate *in vivo*, because RNase G did not efficiently cleave this substrate *in vitro* either (Kim, K., unpublished observations).

NTH-RNase E preferred G/C to A/U as the first nucleotide of the *rne*-dependent site of p23 RNA. This result is rather surprising, since RNase E is known to prefer A/U-rich sequences for recognition (*16–18*, *30*). Furthermore, this result differs from the data of the oligonucleotide-based assay that the C substitution does not cause cleavage (*38*). This difference may imply that NTH-RNase E differentially recognizes oligonucleotides and natural substrates.

The high K_m values for better substrates may be associated with the possibility that the product release becomes rate-limiting in our NTH-RNase E reaction conditions. In this case, the measured k_{cat} could be defined by the magnitude of the rate constant for dissociation of the enzyme-product complex. Since the value of the rate constant for dissociation of the enzyme-product complex is close to that for dissociation of the enzyme-substrate complex, higher K_m would lead to higher observed k_{cat}. However, we did not find a linear relationship between the two parameters. Therefore, it is unlikely that the simultaneous change of K_m and k_{cat} values simply results from rate limiting of the product release in the NTH-RNase E reaction. An alternative explanation is that ES complexes with higher K_m values would be at higher energies than those with lower K_m values if K_m is treated as an apparent dissociation constant of the enzyme-substrate complex (*39*). In this case, high K_m values would result in the enzyme-substrate complex being a "step up the thermodynamic ladder," as suggested by Fersht (*39*). The high K_m value for more specific substrates may reflect the lack of specific binding ability of NTH-RNase E to target RNA molecules and consequently the requirement of the arginine-rich domain of RNase E for the specific binding (*37*).

This work was supported by the 21C Frontier Microbial Genomics and Application Center Program (MG02-0201-003), the Molecular and Celluar BioDiscovery Research Program (2004-01711), and the Basic Research Program (R01-1999-000-00115-0) of KOSEF.

REFERENCES

1. Ghora, B.K. and Apirion, D. (1978) Structural analysis and *in vitro* processing to p5S rRNA of a 9S RNA molecule isolated from an *rne* mutant of *E. coli*. *Cell* **15**, 1055–1066
2. Casaregola, S., Jacq, A., Laoudj, D., McGurk, G., Margarson, S., Tempete, M., Norris, V., and Holland, I.B. (1992) Cloning and analysis of the entire *Escherichia coli ams* gene. ams is identical to hmp1 and encodes a 114 kDa protein that migrates as a 180 kDa protein. *J. Mol. Biol.* **228**, 30–40
3. Casaregola, S., Jacq, A., Laoudj, D., McGurk, G., Margarson, S., Tempete, M., Norris, V., and Holland, I.B. (1994) Cloning and analysis of the entire *Escherichia coli ams* gene. ams is identical to hmp1 and encodes a 114 kDa protein that migrates as a 180 kDa protein. *J. Mol. Biol.* **238**, 867
4. Misra, T.K. and Apirion, D. (1979) RNase E, an RNA processing enzyme from *Escherichia coli*. *J. Biol. Chem.* **254**, 11154–11159
5. Babitzke, P. and Kushner, S.R. (1996) The Ams (altered mRNA stability) protein and ribonuclease E are encoded by the same structural gene of *Escherichia coli*. *Proc. Natl Acad. Sci. USA* **88**, 1–5
6. Melefors, O. and von Gabain, A. (1991) Genetic studies of cleavage-initiated mRNA decay and processing of ribosomal 9S RNA show that the *Escherichia coli ams* and *rne* loci are the same. *Mol. Microbiol.* **5**, 857–864
7. Mudd, E.A., Krisch, H.M., and Higgins, C.F. (1990) RNase E, an endoribonuclease, has a general role in the chemical decay of *Escherichia coli* mRNA: evidence that *rne* and *ams* are the same genetic locus. *Mol. Microbiol.* **4**, 2127–2135
8. Taraseviciene, L., Miczak, A., and Apirion, D. (1991) The gene specifying RNase E (*rne*) and a gene affecting mRNA stability (*ams*) are the same gene. *Mol. Microbiol.* **5**, 851–855
9. McDowall, K.J. and Cohen, S.N. (1996) The N-terminal domain of the *rne* gene product has RNase E activity and is non-overlapping with the arginine-rich RNA-binding site. *J. Mol. Biol.* **255**, 349–355
10. McDowall, K.J., Hernandez, R.G., Lin-Chao, S., and Cohen, S.N. (1993) The *ams-1* and *rne-3071* temperature-sensitive mutations in the *ams* gene are in close proximity to each other and cause substitutions within a domain that resembles a product of the *Escherichia coli mre* locus. *J. Bacteriol.* **175**, 4245–4249
11. Taraseviciene, L., Bjork, G.R., and Uhlin, B.E. (1995) Evidence for an RNA binding region in the *Escherichia coli* processing endoribonuclease RNase E. *J. Biol. Chem.* **270**, 26391–26398
12. Kaberdin, V.R., Miczak, A., Jakobsen, J.S., Lin-Chao, S., McDowall, K.J., and von Gabain, A. (1998) The endoribonucleolytic N-terminal half of *Escherichia coli* RNase E is evolutionarily conserved in *Synechocystis sp.* and other bacteria but not the C-terminal half, which is sufficient for degradosome assembly. *Proc. Natl Acad. Sci. USA* **95**, 11637–11642
13. Vanzo, N.F., Li, Y.S., Py, B., Blum, E., Higgins, C.F., Raynal, L.C., Krisch, H.M., and Carpousis, A.J. (1998) Ribonuclease E organizes the protein interactions in the *Escherichia coli* RNA degradosome. *Genes Dev.* **12**, 2770–2781
14. Coburn, G.A. and Mackie, G.A. (1999) Reconstitution of a minimal RNA degradosome demonstrates functional coordination between a 3′ exonuclease and a DEAD-box RNA helicase. *Genes Dev.* **13**, 2594–2603
15. Ehretsmann, C.P., Carpousis, A.J., and Krisch, H.M. (1992) Specificity of *Escherichia coli* endoribonuclease RNase E: *in vivo* and *in vitro* analysis of mutants in a bacteriophage T4 mRNA processing site. *Genes Dev.* **6**, 149–159
16. McDowall, K.J., Lin-Chao, S., and Cohen, S.N. (1994) A+U content rather than a particular nucleotide order determines the specificity of RNase E cleavage. *J. Biol. Chem.* **269**, 10790–10796
17. Lin-Chao, S., Wong, T.T., McDowall, K.J., and Cohen, S.N. (1994) Effects of nucleotide sequence on the specificity of *rne*-dependent and RNase E-mediated cleavages of RNA I encoded by the pBR322 plasmid. *J. Biol. Chem.* **269**, 10797–10803
18. Mackie, G.A. (1991) Specific endonucleolytic cleavage of the mRNA for ribosomal protein S20 of *Escherichia coli* requires the product of the *ams* gene *in vivo* and *in vitro*. *J. Bacteriol.* **173**, 2488–2497
19. Pragai, B. and Apirion, D. (1982) Processing of bacteriophage T4 transfer RNAs. Structural analysis and *in vitro* processing of precursors that accumulate in RNase E-strains. *J. Mol. Biol.* **154**, 465–484
20. Mackie, G.A. (1992) Secondary structure of the mRNA for ribosomeal protein S20. *J. Biol. Chem.* **267**, 1054–1061

21. Mackie, G.A. and Genereaux, J.L. (1993) The role of RNA structure in determining RNase E-dependent cleavage sites in the mRNA for ribosomal protein S20 i*n vitro*. *J. Mol. Biol.* **234**, 998–1012
22. Nilsson, G., Lundberg, U., and von Gabain, A. (1988) *In vivo* and *in vitro* identity of site specific cleavages in the 5′ noncoding region of *ompA* and *bal* mRNAs in *Escherichia coli*. *EMBO J.* **7**, 2269–2275
23. Cormack, R.S. and Mackie, G.A. (1992) Structural requirements for the processing of *Escherichia coli* 5S ribosomal RNA by RNase E *in vitro*. *J. Mol. Biol.* **228**, 1078–1090
24. Mackie, G.A., Genereaux, J.L., and Masterman, S.K. (1997) Modulation of the activity of RNase E *in vitro* by RNA sequences and secondary structures 5′ to cleavage sites. *J. Biol. Chem.* **272**, 609–616
25. McDowall, K.J., Kaberdin, V.R., Wu, S.-W., Cohen, S.N., and Lin-Chao, S. (1995) Site-specific RNase E cleavage of oligonucleotides and inhibition by stem-loops. *Nature* **374**, 287–290
26. Guerrier-Takada, C., Gardiner, K., Marsh, T., Pace, N., and Altman, S. (1983) The RNA moiety of ribonuclease P is the catalytic subunit of enzyme. *Cell* **35**, 849–857
27. Gurevitz, M., Jain, S.K., and Apirion, D. (1983) Identification of a precursor molecular for the RNA moiety of the processing enzyme RNase P. *Proc. Natl Acad. Sci. USA* **80**, 4450–4454
28. Sakamoto, H., Kimura, N., and Shimura, Y. (1983) Processing of transcription products of the gene encoding the RNA component of RNase P. *Proc. Natl Acad. Sci. USA* **80**, 6187–6191
29. Lundberg, U. and Altman, S. (1995) Processing of the precursor to the catalytic RNA subunit of RNase P from *Escherichia coli*. *RNA* **1**, 327–334
30. Kim, S., Kim, H., Park, I., and Lee, Y. (1996) Mutational analysis of RNA structures and sequences postulated to affect 3′ processing of M1 *RNA*, the RNA component of *Escherichia coli* RNase P. *J. Biol. Chem.* **271**, 19330–19337
31. Kim, S., Sim, S., and Lee, Y. (1999) *In vitro* analysis of processing at the 3′-end of precursors of M1 *RNA*, the catalytic subunit of *Escherichia coli* RNase P: multiple pathways and steps for the processing. *Nucleic Acids Res.* **27**, 895–901
32. Sim, S., Kim, K., and Lee, Y. (2002) 3′-end processing of precursor M1 RNA by the N-terminal half of RNase E. *FEBS Lett.* **529**, 225–231
33. Sim, S., Kim, S., and Lee, Y. (2001) Role of the sequence of the *rne*-dependent site in 3′ processing of M1 RNA, the catalytic component of *Escherichia coli* RNase P. *FEBS Lett.* **505**, 291–295
34. Yanisch-Perron, C., Vieira, J., and Messing, J. (1985) Improved M13 phage cloning vectors and host strains: nucleotide sequences of the M13mp18 and pUC19 vectors. *Gene* **33**, 103–119
35. Studier, F.W., Rosenberg, A.H., Dunn, J.J., and Dubendorff, J.W. (1990) Use of T7 RNA polymerase to direct expression of cloned genes. *Methods Enzymol.* **185**, 60–89
36. Sambrook, J. and Russel, D.W. (2001) *Molecular Cloning: A Laboratory Manual*, 3rd ed., Cold Spring Harbor Laboratory Press, Cold Spring Harbor, NY
37. Kaberdin, V.R., Walsh, A.P, Jakobsen, T., McDowall, K.J., and von Gabain, A. (2000) Enhanced cleavage of RNA mediated by an interaction between substrates and the arginine-rich domain of *E. coli* ribonuclease E. *J. Mol. Biol.* **301**, 257–264
38. Kaberdin, V.R. (2003) Probing the substrate specificity of *Escherichia coli* RNase E using a novel oligonucleotide-based assay. *Nucl. Acids Res.* **31**, 4710–4716
39. Fersht, A.R. (1974) Catalysis, binding and enzyme-substrate complementarity. *Proc. R. Soc. Lond. B Biol. Sci.* **187**, 397–407